

## Supporting Information

### **High Quality Borophene Quantum Dots Realization and their Application in Photovoltaic Device**

Anran Zhao<sup>ac</sup>, Yu Han<sup>bc</sup>, Yuhang Che<sup>bc</sup>, Qi Liu<sup>ac</sup>, Xiyang Wang<sup>d</sup>, Qi Li<sup>ac</sup>, Jie Sun<sup>ac</sup>,  
Zhibin Lei<sup>ac</sup>, Xuexia He<sup>\*ac</sup> and Zong-Huai Liu<sup>\*ac</sup>

a. Key Laboratory of Applied Surface and Colloid Chemistry (Shaanxi Normal

University), Ministry of Education, Xi'an, 710062, P. R. China. E-mail:

xxhe@snnu.edu.cn; zhliu@snnu.edu.cn

b. Shaanxi Key Laboratory for Advanced Energy Devices; Xi'an, 710119, P. R. China

c. School of Materials Science and Engineering, Shaanxi Normal University, Xi'an,

710119, P. R. China

d. State Key Laboratory of Inorganic Synthesis and Preparative Chemistry,

International Joint Research Laboratory of Nano-Micro Architecture Chemistry,

College of Chemistry, Jilin University, Changchun, 130012, P. R. China

Firstly, bulk B precursors are grounded in a mortar for 30 minutes, making it partly exfoliate and thin along the direction of layered horizontally. Secondary, the thinned B precursors are dispersed into a mixed solution of N-methyl pyrrolidone (NMP) and butyl alcohol (NBA) and stirred for 12 hours at a speed of 400 rpm, a transparent dispersion is obtained. Then it is probe sonicated for 6 h in an ice-bath, an intermediate consisted of BQDs and borophene with few-layers and relatively small size is obtained. Thirdly, the intermediate is bath ultrasound treated for 2 h at a power of 600 W, and the obtained dispersion is centrifuged under 7000 rpm for 20 min, BQDs with a lateral size of 4 nm and a thickness of about 2 nm are finally prepared. Research results indicate that borophene with few-layers and large size can be obtained in a short time when NMP solvent is only used.<sup>1</sup> While using a two-solvent system of NMP/NBA to treat B bulk precursors, the mixing enthalpy of the system plays a leading role, and the hydrogen bond existed in the system makes the intercalated molecules occupy a larger space range and causes the van der Waals force between B layers easier overcome, greatly improving the stripping efficiency and the stability of the obtained dispersion.

The probe sonication power and time are important controlling factors for QDs preparation from its native layered precursors. If the ultrasonic energy for probe sonication is high enough, the ultrasonic cavitation will greatly increase the rate of heterogeneous reaction and realize the uniform mixing between heterogeneous reactions, favourable for the size and distribution control of the obtained QDs.<sup>2</sup> In order to investigate the effect of the probe sonication power and time on the size, uniform, and distribution of the obtained BQDs, different probe sonication times at a power of 600 W are selected to observe the influence, and the experimental results are shown in Figure S2. TEM images of the obtained BQDs with different resolutions at different probe times show that their size and uniform are connected with the probe time. Although BQDs can be obtained at different probe sonication times, their size, uniform, and distribution are changed with the probe sonication time. By prolonging the probe sonication time, the size of the obtained BQDs is gradually decreased. Moreover, from the size distribution analyses of the obtained BQDs at different probe

sonication times, it can be seen that although BQDs with 3-4 nm can be prepared, the particle size is relatively uniform and the size distribution is very closer to the normal distribution when the probe sonication time is 6 h.

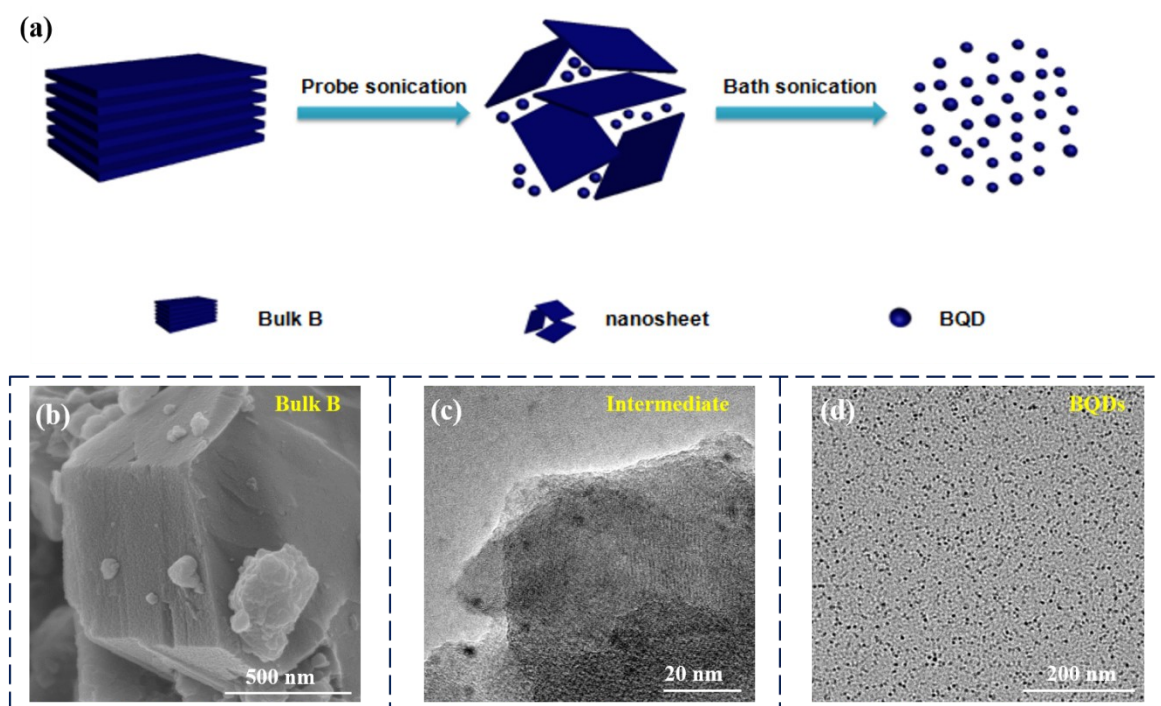
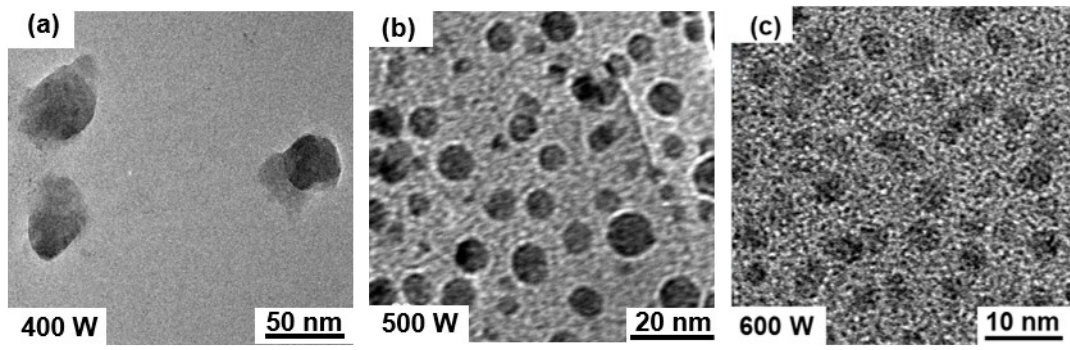


**Figure S1.** Schematic illustration of the preparation of BQDs obtained by grinding assisted probe ultrasonic treatment in a mixture solvent of NMP and NBA (a), SEM image of bulk B (b), TEM images of intermediate (c) and BQDs (d).



**Fi**

**Figure S2.** TEM morphologies of BQDs with different sonication power treatment in a mixture solvent of NMP and NBA (a) 400 w, (b) 500 w, and (c) 600 w, respectively

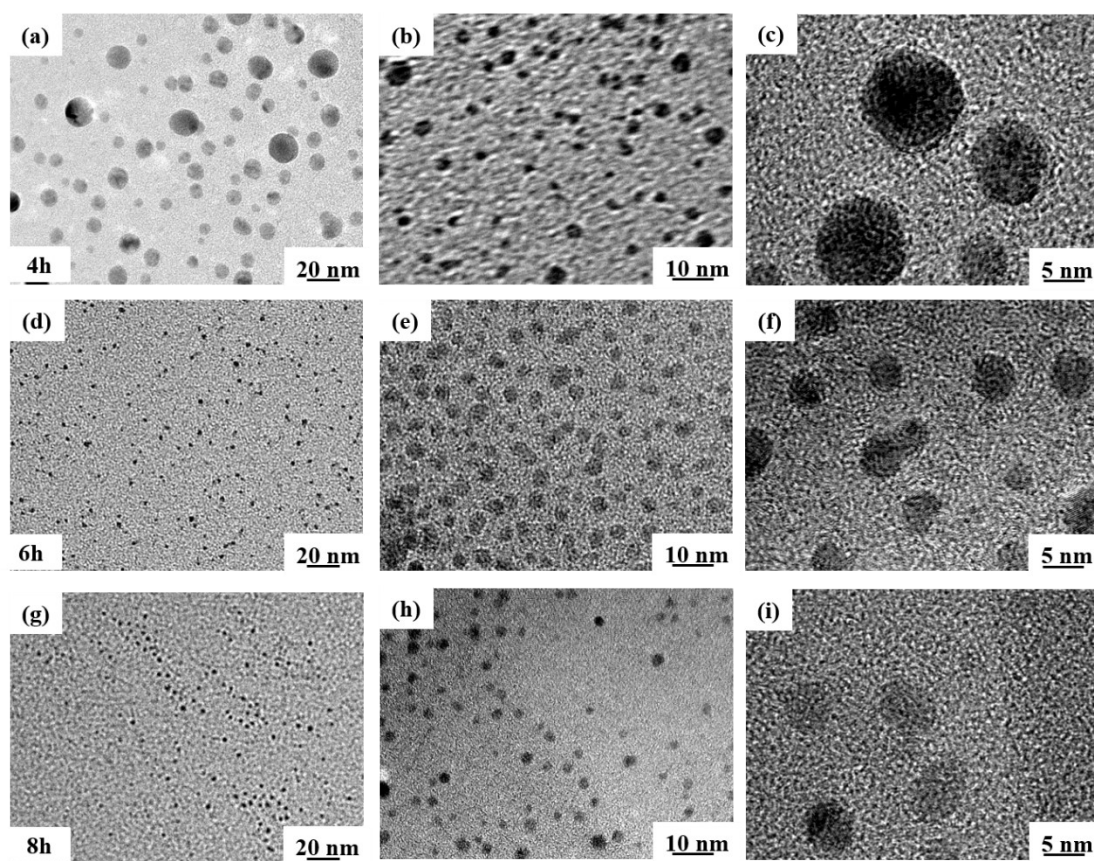


**Figure S3.** TEM morphologies with different resolutions of BQDs with different sizes obtained by grinding assisted probe ultrasonic treatment in a mixture solvent of NMP and NBA for different times: (a-c) 4h, (d-f) 6h, and (g-i) 8h, respectively.

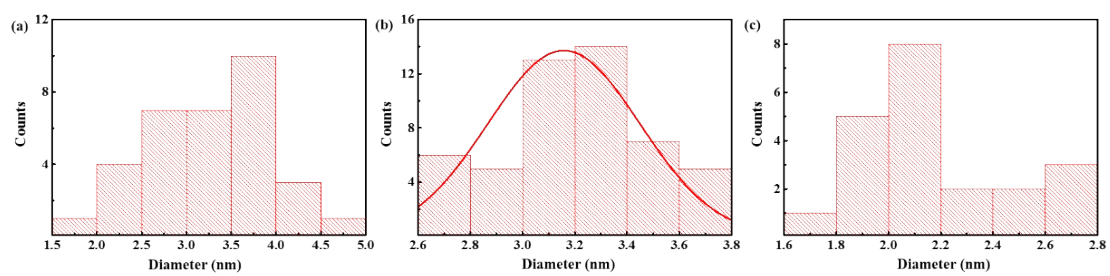


**Figure S4.** Dynamic Light Scattering of BQDs obtained by probe ultrasonic treatment for different time: (a) 4 h, (b) 6 h, and (c) 8 h.

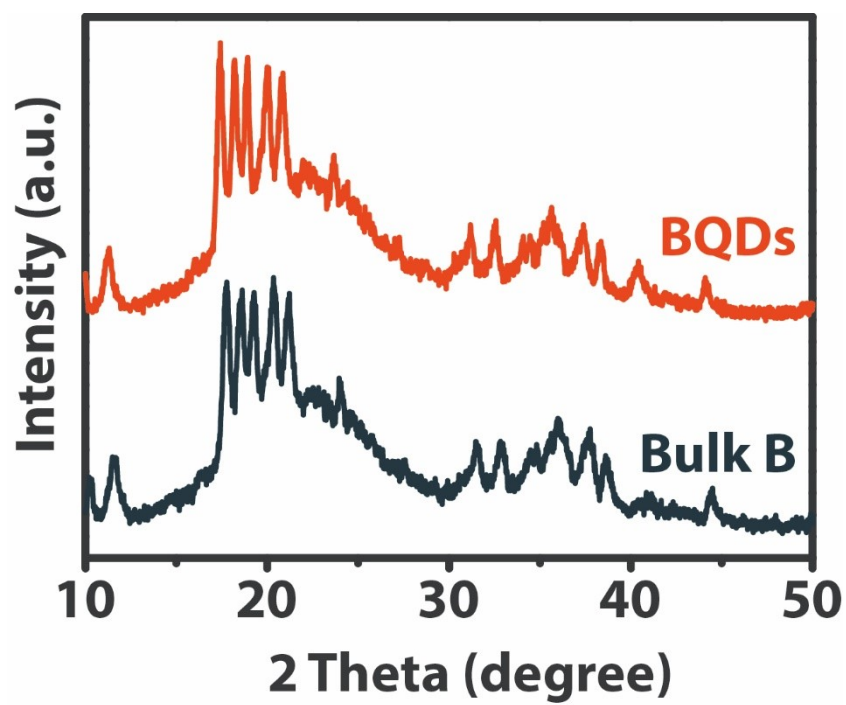


**Figure S5.** XRD patterns of bulk B and BQDs obtained by grinding assisted probe ultrasonic treatment in a mixture solvent of NMP and NBA for 6 h.



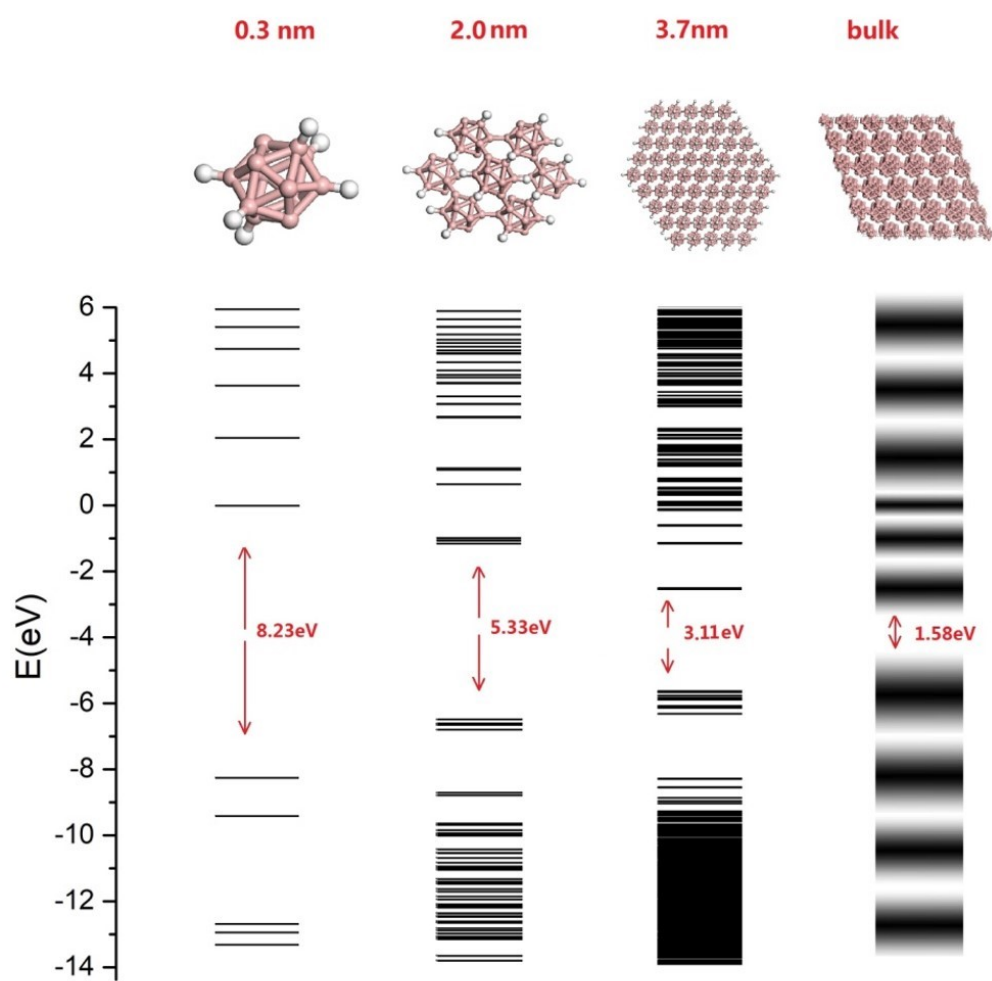


**Figure S6.** First-principles DFT calculations of band gap for size for BQDs increases from 0.3 nm to 2.0 nm to 3.7 nm to  $\infty$  (bulk).

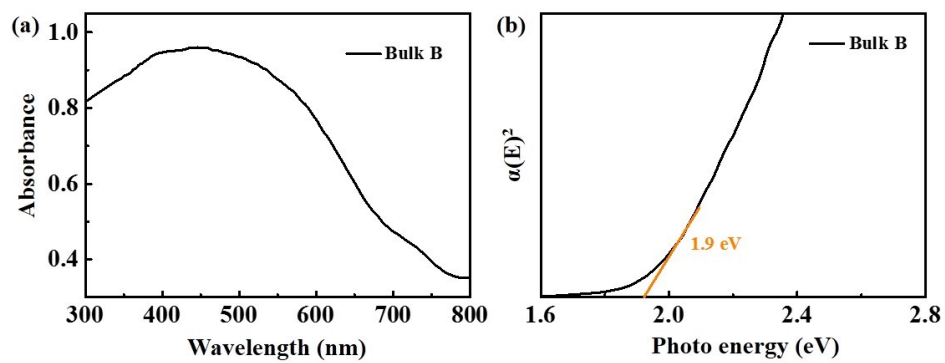


**Figure S7.** UV-Vis absorption spectrum of bulk boron (a) and corresponding optical band gap (b).

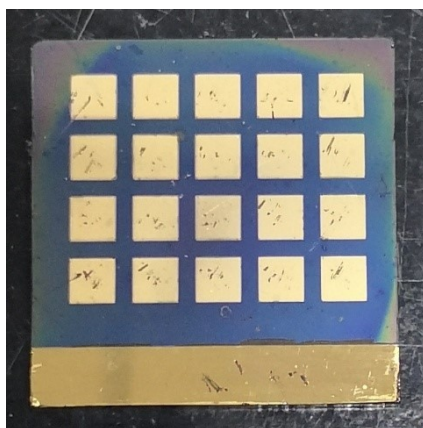


**Figure S8.** The schematic diagram of the device.

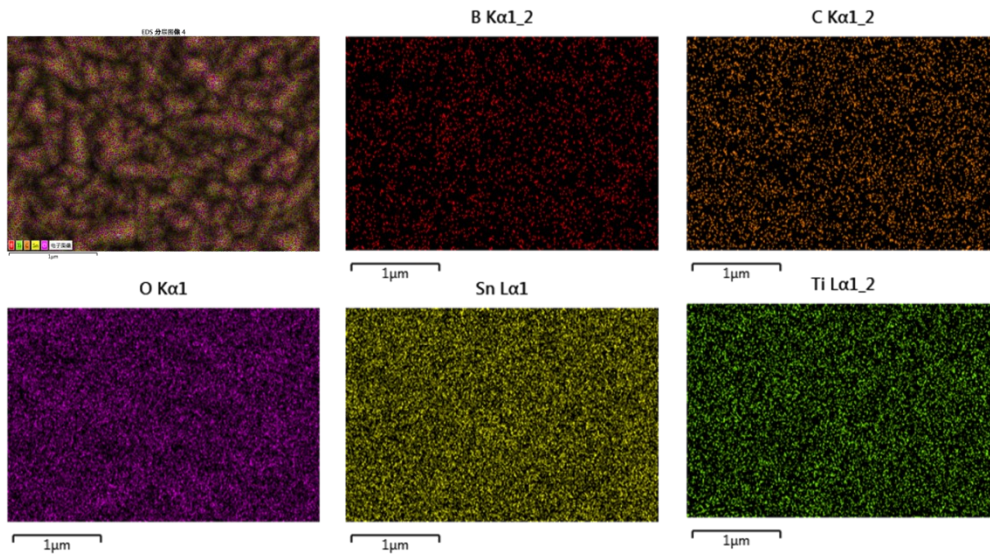


**Figure S9.** SEM images for a top-view region and the corresponding B, C, O, Sn, and Ti elemental mappings.

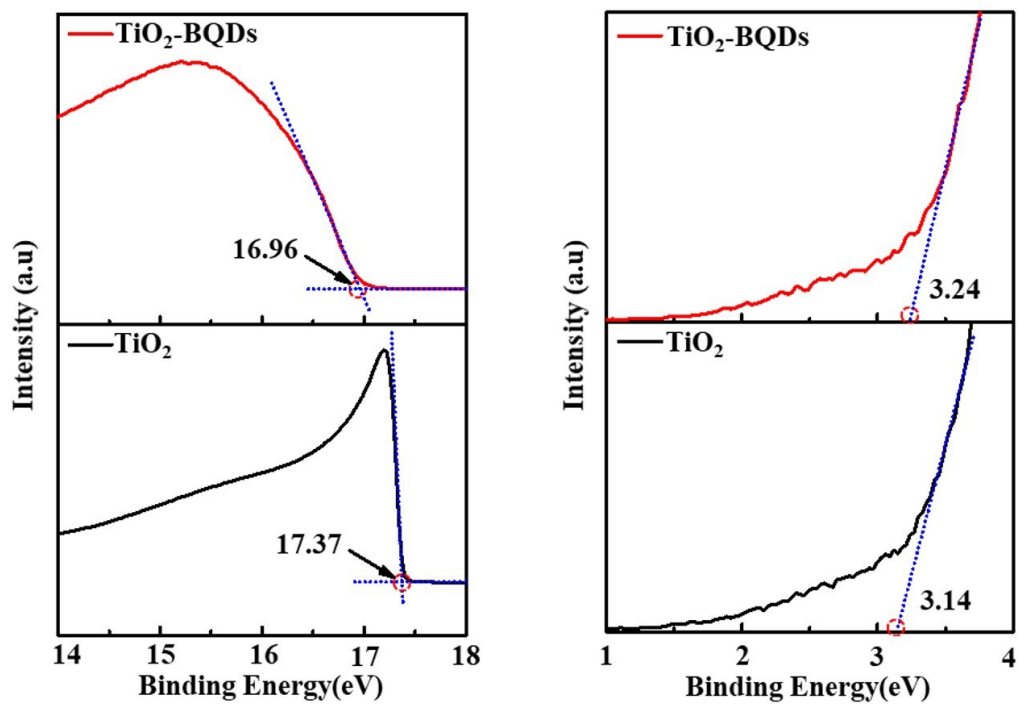


**Figure S10.** Ultraviolet photoelectron spectroscopy spectra of TiO<sub>2</sub> and TiO<sub>2</sub> modified by BQDs.

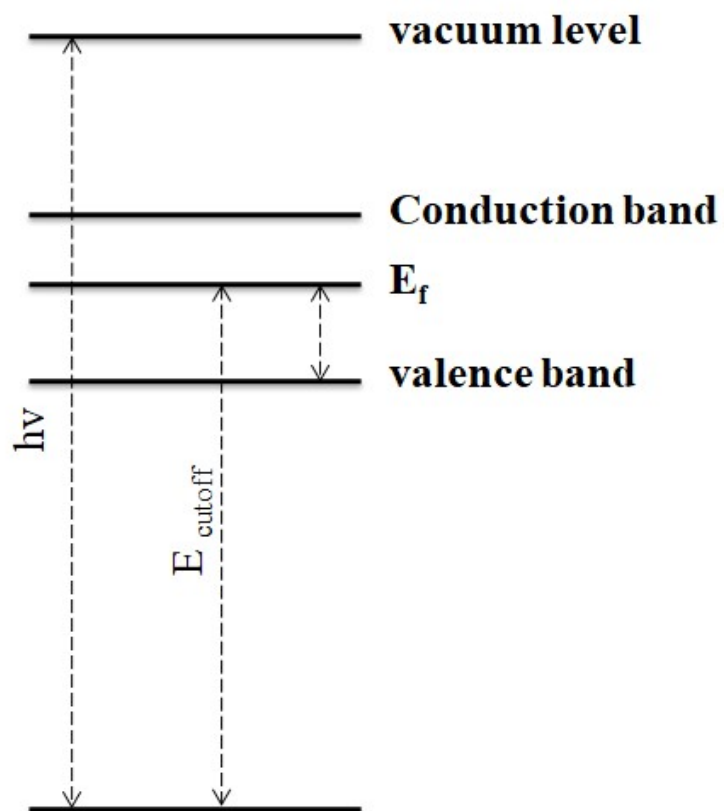


**Figure S11.** Band diagram of the energy level of EVBM,  $E_{\text{cutoff}}$ , and  $E_f$

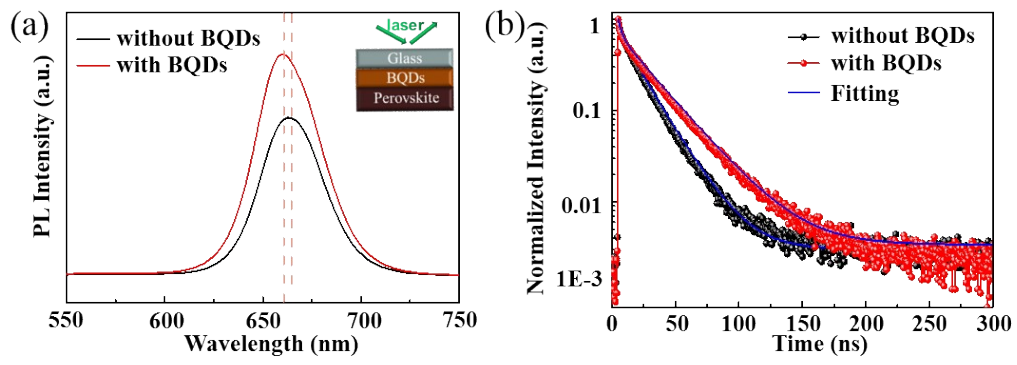


**Figure S12.** (a) Steady-state PL spectra and (b) time-resolved PL spectra of CsPbI<sub>2</sub>Br films without and with BQDs.

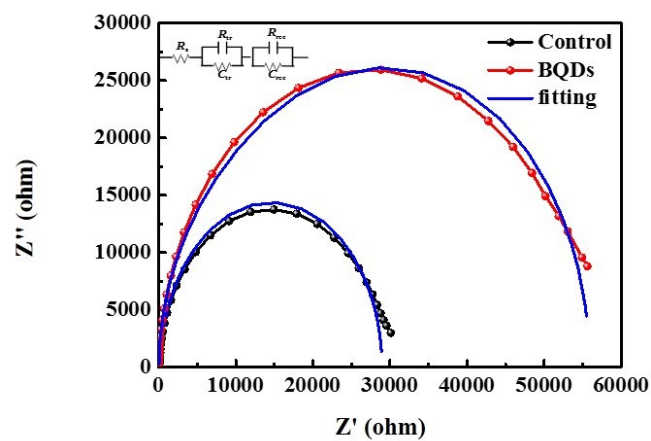


**Figure S13.** Nyquist plots of the control and optimized CsPbI<sub>2</sub>Br PSCs; the inset depicts the equivalent circuit employed to fit the Nyquist plots.



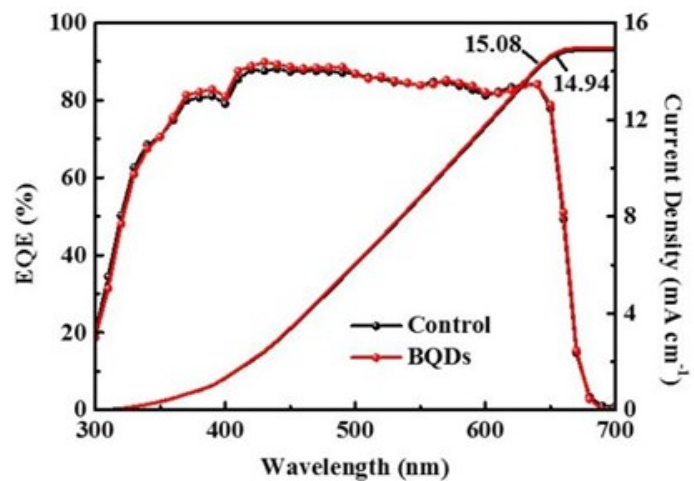


**Figure S14.** EQE spectra of the CsPbI<sub>2</sub>Br PSCs without and with 0.01 mg/mL BQDs.

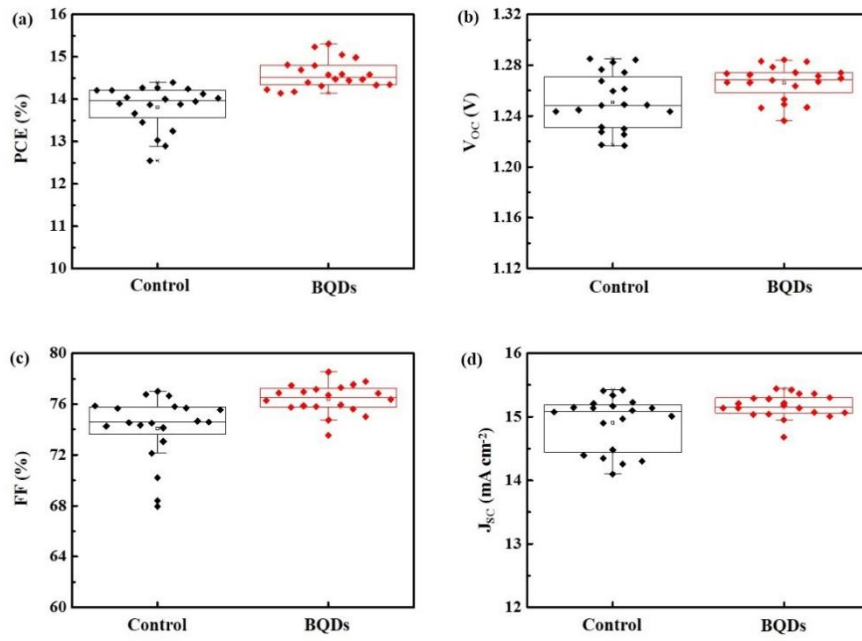


**Figure S15.** Statistic distributions of (a) PCE and (b)  $V_{oc}$  and (c) FF and (d)  $J_{sc}$  for the CsPbI<sub>2</sub>Br PSCs without and with 0.01 mg/mL BQDs.

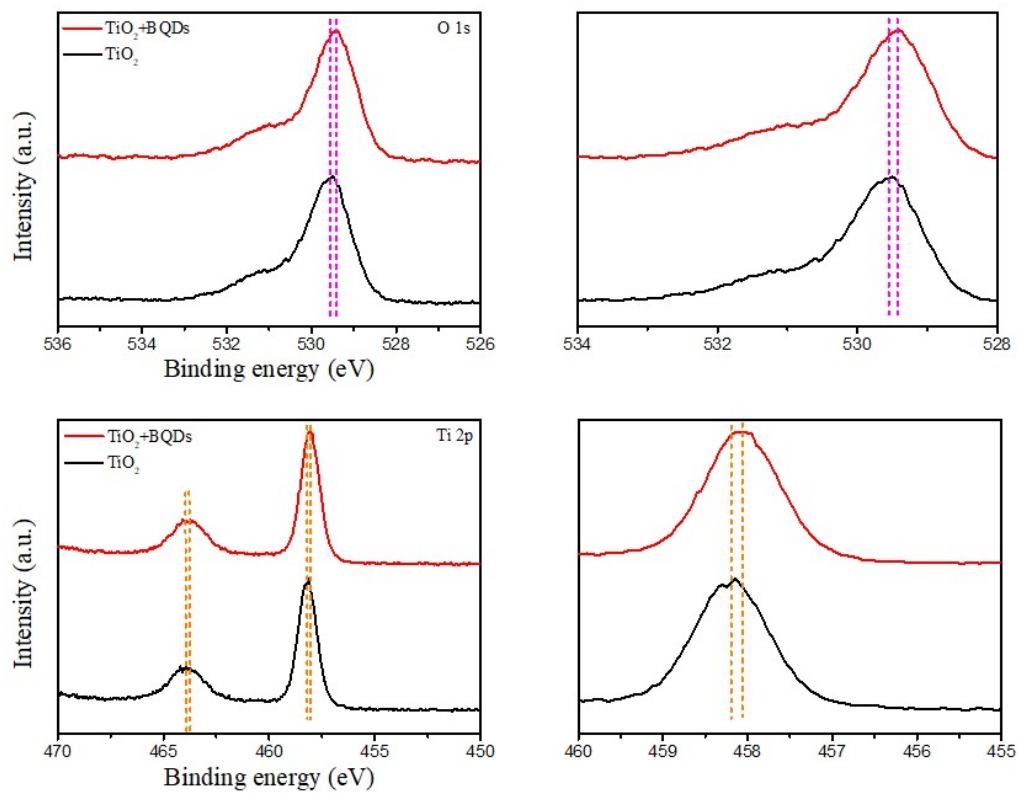


**Figure S16.** XPS O 1s and Ti 2p spectra of TiO<sub>2</sub> films without and with BQDs.

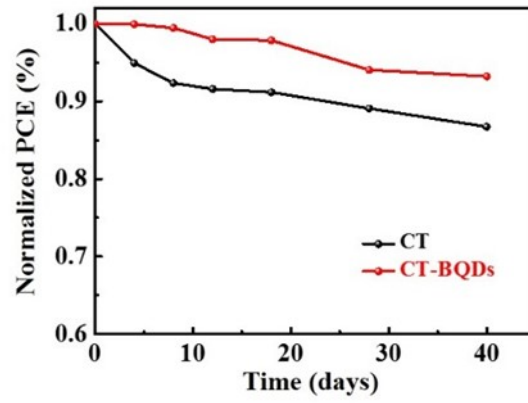


**Figure S17.** The air stability (humidity:~20%) of CsPbI<sub>2</sub>Br PSCs without and with BQDs treatment.

**Table S1.** Fitting parameters of the PL decay spectra for CsPbI<sub>2</sub>Br films without and with 0.01mg/mL BQDs on TiO<sub>2</sub>.

Samples	$\tau_{ave}$ (ns)	$\tau_1$ (ns)	A <sub>1</sub> (%)	$\tau_2$ (ns)	A <sub>2</sub> (%)
without BQDs	11.84	16.83	44.25	7.88	55.75
0.01mg/mL BQDs	6.50	14.17	12.58	5.45	87.42

**Table S2.** Fitting parameters of the PL decay spectra for CsPbI<sub>2</sub>Br films without and with BQDs on glass.

Samples	$\tau_{ave}$ (ns)	$\tau_1$ (ns)	A <sub>1</sub> (%)	$\tau_2$ (ns)	A <sub>2</sub> (%)
without BQDs	17.24	18.71	89.57	4.61	10.43
with BQDs	25.82	26.95	66.76	2.64	33.64

**Table S3.** Fitted EIS parameters for the control and optimized CsPbI<sub>2</sub>Br PSCs.

Sample	R <sub>s</sub> ( $\Omega$ )	R <sub>tr</sub> ( $\Omega$ )	C <sub>tr</sub> (F)	R <sub>rec</sub> ( $\Omega$ )	C <sub>rec</sub> (F)
without BQDs	80.45	1907	$3.88 \times 10^{-8}$	28690	$6.65 \times 10^{-9}$
with BQDs	51.98	7966	$1.61 \times 10^{-8}$	47860	$9.34 \times 10^{-9}$

1. Li, H.; Jing, L.; Liu, W.; Lin, J.; Tay, R. Y.; Tsang, S. H.; Teo, E. H. T., Scalable production of few-layer boron sheets by liquid-phase exfoliation and their superior supercapacitive performance. *ACS Nano* **2018**, *12* (2), 1262-1272.
2. Li, H.; He, X.; Liu, Y.; Yu, H.; Kang, Z.; Lee, S.-T., Synthesis of fluorescent carbon nanoparticles directly from active carbon via a one-step ultrasonic treatment. *Mater. Res. Bull.* **2011**, *46* (1), 147-151.